NEOPLASIA
www.neoplasia.com

Volume 16 Number 12 December 2014 pp. 1047–1058 1047

# Suppression of Invasion and Metastasis of Triple-Negative Breast Cancer Lines by Pharmacological or Genetic Inhibition of Slug Activity[1,2,3]

**Giovanna Ferrari-Amorotti*, Claudia Chiodoni†, Fei Shen‡, Sara Cattelani*, Angela Rachele Soliera*, Gloria Manzotti*, Giulia Grisendi§, Massimo Dominici§, Francesco Rivasi¶, Mario Paolo Colombo†, Alessandro Fatatis‡,#,** and Bruno Calabretta*,††**

*Dipartimento di Medicina Diagnostica, Clinica a di Sanità Pubblica, University of Modena and Reggio Emilia, Modena, Italy; †Istituto Tumori Milano, Milano, Italy; ‡Department of Pharmacology and Physiology, Drexel University, Philadelphia, PA, USA; §Dipartimento di Scienze Mediche e Chirurgiche Materno-Infantili e dell'Adulto, Modena, Italy; ¶Dipartimento di Anatomia Patologica e Medicina Legale, University of Modena and Reggio Emilia, Modena, Italy; #Department of Pathology, Drexel University, Philadelphia, PA, USA; **Program in Biology of Prostate Cancer, Kimmel Cancer Center, Philadelphia, PA, USA; ††Department of Cancer Biology and Kimmel Cancer Center, Thomas Jefferson University, Philadelphia, PA, USA

## Abstract

Most triple-negative breast cancers (TNBCs) exhibit gene expression patterns associated with epithelial-to-mesenchymal transition (EMT), a feature that correlates with a propensity for metastatic spread. Overexpression of the EMT regulator Slug is detected in basal and mesenchymal-type TNBCs and is associated with reduced E-cadherin expression and aggressive disease. The effects of Slug depend, in part, on the interaction of its N-terminal SNAG repressor domain with the chromatin-modifying protein lysine demethylase 1 (LSD1); thus, we investigated whether tranylcypromine [also known as trans-2-phenylcyclopropylamine hydrochloride (PCPA) or Parnate], an inhibitor of LSD1 that blocks its interaction with Slug, suppresses the migration, invasion, and metastatic spread of TNBC cell lines. We show here that PCPA treatment induces the expression of E-cadherin and other epithelial markers and markedly suppresses migration and invasion of TNBC cell lines MDA-MB-231 and BT-549. These effects were phenocopied by Slug or LSD1 silencing. In two models of orthotopic breast cancer, PCPA treatment reduced local tumor growth and the number of lung metastases. In mice injected directly in the blood circulation with MDA-MB-231 cells, PCPA treatment or Slug silencing markedly inhibited bone metastases but had no effect on lung infiltration. Thus, blocking Slug activity may suppress the metastatic spread of TNBC and, perhaps, specifically inhibit homing/colonization to the bone.

*Neoplasia (2014) 16, 1047–1058*

Address all correspondence to: Giovanna Ferrari-Amorotti, PhD, Via Campi 287, 41125 Modena, Italy; Bruno Calabretta, MD, PhD, 233 S. 10th Street, Philadelphia, PA 19106. E-mail: ferrariamorotti@hotmail.it

[1] Financial support: This work was supported by grants from the "Associazione Nuova Vita onlus" and Fondazione Cassa di Risparmio di Vignola and by National Cancer Institute grants RO1CA167169 (B.C.) and R21CA178540 (A.F.). G.F.-A. was supported by a fellowship from the Fondazione Umberto Veronesi. A.R.S. and G.M. are supported by a fellowship from Associazione Italiana per la Ricerca sul Cancro. S.C. was supported by a fellowship from "Associazione Marta Nurizzo" and is currently supported by a fellowship from the Fondazione Umberto Veronesi. M.P.C. is supported by a grant from Associazione Italiana per la Ricerca sul Cancro (IG-2013 14194).

[2] Disclosure of potential conflicts of interest: No potential conflicts of interests were disclosed.

[3] This article refers to supplementary materials, which is designated by Supplementary Figures 1 to 5 and are available online at www.neoplasia.com.

Received 17 June 2014; Revised 10 October 2014; Accepted 13 October 2014



1476-5586/14
http://dx.doi.org/10.1016/j.neo.2014.10.006

## Introduction

Treatment of breast cancer has substantially improved over the past 30 years due, in large part, to the development of more effective combination chemotherapy protocols, endocrine therapies, and human epidermal growth factor receptor 2–targeted therapies [1–4]. However, progress of patients with triple-negative breast cancer (TNBC), which are estrogen receptor–, progesterone receptor–, and human epidermal growth factor receptor 2–negative and represent 10% to 15% of the total, has been more limited because they cannot be treated with endocrine or targeted therapies. Although TNBC is histopathologically heterogeneous, the vast majority are high-grade invasive ductal carcinomas characterized by marked degrees of nuclear pleomorphism, lack of tubule formation, high number of mitotic cells, and high frequency of p53 mutations [5,6]. Microarray-based analysis of TNBCs has identified six reproducible gene expression subtypes, two of which, the mesenchymal-like and the mesenchymal stem–like, show enrichment for gene expression patterns associated with epithelial-to-mesenchymal transition (EMT) [7]. Such enrichment correlates with a propensity of TNBC cells to disseminate as indicated by increased expression of EMT markers in breast cancer circulating tumor cells (CTCs) [8]. The EMT is a process through which tumor cells lose homotypic adhesion, change morphology, and acquire migratory and invasive capacity [9,10]. EMT is thought to contribute to tumor progression, and aberrant expression of EMT regulator/inducers in cancer cells correlates with tumor aggressiveness and poor clinical outcomes [11]. Transcriptional repression of E-cadherin expression is a key event during EMT. The human E-cadherin promoter contains E-box elements that are required for regulation of its transcription [12]. The zinc-finger transcription factors (TFs) Snail [13], Slug [14], Zeb1 [15], and Zeb2 [16] can bind directly to these E-boxes and repress E-cadherin transcription. Slug contributes to invasion in many tumor types [17–20] and can cooperate with Twist or Sox9 in promoting invasion and metastasis [21,22]. Overexpression of Slug is detected in many tumors [23] including the basal and mesenchymal-type TNBCs [7,24,25] and is associated with reduced E-cadherin expression, high histologic grade, lymph node metastasis, post-operative relapse, and shorter patients' survival [26–28]. Moreover, Slug represses the expression of E-cadherin and of the cell-cell junction protein plakoglobin in TNBC cells [15,29] and its silencing suppresses the invasion of breast cancer cells [30].

Because Slug-regulated transcription repression depends, in part, on the interaction of its N-terminal SNAG repressor domain with chromatin-modifying proteins such as lysine demethylase 1 (LSD1) [31,32], inhibitors of this interaction may suppress the motility and invasion of TNBC cells. A previous study from our laboratories has shown that treatment with tranylcypromine [also known as trans-2-phenylcyclopropylamine hydrochloride (PCPA) or Parnate], an Food and Drug Administration-approved monoamine oxidase (MAO)/LSD1 enzymatic inhibitor [33], or TAT-SNAG, a cell permeable peptide that includes the highly conserved SNAG domain of Slug, blocks Slug-dependent repression of the E-cadherin promoter, suppresses the expression of morphologic and molecular markers of EMT, and inhibits the motility and invasion of tumor cells of different histologic and genetic backgrounds [34].

In this study, we extended these findings to investigate the effects of PCPA and the requirement of Slug or LSD1 expression for the migration, invasion, and EMT marker expression of TNBC cell lines *in vitro* and for metastatic spread in mouse models of TNBC.

We show here that TNBC cell lines MDA-MB-231 and BT-549 are highly dependent on Slug/LSD1 activity for their migration and invasion and that treatment with PCPA has anti-metastatic effects in orthotopic models of breast cancer and in immunodeficient mice injected intracardiacally with TNBC MDA-MB-231 cells.

## Materials and Methods

### *Plasmids and Antibodies*

TNBC cell lines were lentivirally transduced with the following plasmids: pLKO-SCR-sh and pLKO-Slug-sh [34] and pLKO-Twist2-sh and pGIPZ-LSD1-sh-H6 (purchased from Open Biosystems, Lafayette, CO).

Slug, LSD1, and anti–β-actin expression in transduced cell lines was detected by anti-Slug (Abgent, San Diego, CA; #AP2053a), anti-LSD1 (Abcam, Cambridge, UK; #ab17721), and anti–β-actin (Santa Cruz Biotechnology, Santa Cruz, CA; #sc-47778) antibodies.

### *Cell Lines and Treatments*

Triple-negative mesenchymal-like human breast cancer MDA-MB-231 and BT-549 [7] and 4T1 (murine animal model for stage IV human breast cancer) cell lines were cultured in Dulbecco's modified Eagle's medium (DMEM; Invitrogen, Carlsbad, CA) supplemented with 10% heat-inactivated FBS, 100 units/ml penicillin, 0.1 mg/ml streptomycin, and 2 mM L-glutamine at 37 °C and 5% $CO_2$. Cell lines were obtained from American Type Culture Collection (ATCC, Manassas, VA) and characterized by DNA fingerprinting and isozyme detection. For *in vivo* experiments, cells were engineered to stably express enhanced green fluorescent protein (copGFP) using a lentiviral vector (pCDH-CMV-MCS-EF1-copGFP, SBI). Cells were treated with 100 μM PCPA, a non-selective MAO-A/B/LSD1 inhibitor. All lines were tested for mycoplasma contamination (PCR Mycoplasma Detection Set; Takara Bio Inc, Otsu, Shiga, Japan) every 3 months.

### *Proliferation Assay*

Cell proliferation assay was performed using CellTiter 96 AQueous One Solution Cell Proliferation Assay (Promega, Madison, Wisconsin). Briefly, 5000 cells were seeded in 96-well flat bottom culture plates in 100 μl of culture medium. After 24, 48, 72, and 96 hours, 20 μl of 3-(4,5-dimethylthiazol-2-yl)-5-(3-carboxymethoxyphenyl)-2-(4-sulfophenyl)-2H-tetrazolium solution was added to each well and plates were incubated for 3 hours in a humidified 5% $CO_2$ atmosphere. Absorbance at 492 nm was recorded using a 96-well plate reader. Proliferation of MDA-MB-231 and BT-549 cells was also measured by trypan blue exclusion. Each treatment was performed in triplicate, and the experiment was repeated at least twice.

### *Migration and Invasion Assay*

For wound-healing assays, cells were plated to confluence onto a six-well plate and the cell surface was scratched using a pipette tip. Then, cells were treated with PCPA (100-500 μM), allowed to repopulate the scratched area for 1 to 3 days, and photographed using a digital camera mounted on an inverted microscope (magnification, ×5). Accurate wound measurements were taken at 0 and 72 hours to calculate the migration rate according to the equation: %wound healing = [(wound length at 0 hour) − (wound length at 72 hours)]/(wound length at 0 hour) × 100. Experiments were performed twice independently.

For invasion assays, cells were plated ($10^5$ cells per chamber) onto BD BioCoat Matrigel invasion chambers (BD Biosciences, San Josè,

CA). In the upper chamber, the medium was supplemented with 2% heat-inactivated FBS. In the lower chamber, 20% FBS was used as a chemoattractant. PCPA was added in the upper chamber. After 24 hours, the medium was removed and the chambers were washed twice with phosphate-buffered saline (PBS); non-invading cells were removed from the upper surface of the membrane by scrubbing with a cotton-tipped swab; invading cells were fixed with 3.7% formaldehyde in PBS for 2 minutes, washed twice with PBS, permeabilized with methanol for 20 minutes, washed twice with PBS, stained with 0.05% crystal violet for 15 minutes, and washed twice with PBS. Ten fields for each chamber were photographed using a digital camera mounted on an inverted microscope (magnification, ×10), and invading cells were counted in each field. Experiments were carried out in duplicate and repeated twice.

### *Real-Time Quantitative Polymerase Chain Reaction Analyses*

For real-time quantitative polymerase chain reaction (qPCR), total RNA was isolated from PCPA-treated cells using the RNeasy Mini Kit (Qiagen, Venlo, Netherlands). After digestion with RNase-free DNase (Roche Applied Science, Penzberg, Germany), RNA (4 μg) was reverse-transcribed using SuperScript III Reverse Transcriptase Kit (Invitrogen, Carlsbad, CA), and first-strand cDNA used as a PCR template. Reactions were done in triplicate, and RNA was extracted from two separate experiments.

Primer pairs of analyzed genes (*desmoplakin*: FW 5′-gctaaacgccgccaggat-3′, RV 5′-ccgcatgactgtgttggaat-3′; *occludin*: FW 5′-gccggttcctgaagtggtt-3′, RV 5′-cgaggctgcctgaagtcatc-3′; *E-cadherin*: FW 5′-ccgctggcgtctgtaggaagg-3′, RV 5′-ggctctttgaccaccgctctcc-3′; *N-cadherin*: FW 5′-ctgtgggaatccgacgaatgg-3′, RV 5′-gtcattgtcagccgctttaagg-3′; *vimentin*: FW 5′-ccagccgcagcctctacg-3′, RV 5′-gcgagaagtccaccgagtcc-3′; *plakoglobin*: FW 5′-aaggtgctatccgtgtgtcc-3′, RV 5′-gttgttgcatgtcaggttgg-3′; *huHPRT*: FW 5′-agactttgctttccttggtcagg-3′, RV 5′-gtctggcttatatccaacacttcg-3′; *huTwist*: FW 5′-gtcctccagagcgacgag-3′, RV 5′-agaccgagaaggcgtagc-3′; *ZEB1*: FW 5′-actcagcctcctccactc-3′, RV 5′-acaaattgccatctccagt-3′; *ZEB2*: FW 5′-ggagcaggtaatcgcaagt-3′, RV 5′-cgcaggtgttctttcagatg-3′; *huSnail*: FW 5′-cccaatcggaagcctaa-3′, RV 5′-cctttcccactgtcctcat-3′; *MusM desmoplakin*: FW 5′-gcaacaagcccattatcc-3′, RV 5′-gcaagaaaggtccacagc-3′; *MusM occludin*: 5′-atccacctatcacttcaga-3′, RV 5′-taatctcccaccatcctc 3′; *MusM E-cadherin*: FW 5′-gtctcctcatggctttgc-3′, RV 5′-ctttagatgccgcttcac-3′; *MusM N-cadherin*: FW 5′-gcctatgaaggaaccacatga-3′, RV 5′-ctgtatctcagggaaaggt-3′; *MusM vimentin*: FW 5′-tgtgaggtggagcgggac-3′, RV 5′-acatcgatctggacatgctg-3′; *MusMSnail*: FW 5′-ccactgcaaccgtgcttt-3′, RV 5′-cttggtgcttgtggagcaa-3′; *MusMTwist*: FW: 5′-gccaggtacatcgacttcc-3′, RV 5′-cagcttgccatcttggagt-3′; *MusM glyceraldehyde-3-phosphate dehydrogenase*: FW 5′-gttgtctcctgcgacttca-3′, RV 5′-ggtggtccagggtttctta-3′) were designed using Beacon Design software. Real-time qPCR was performed using GoTaq qPCR Master Mix (Promega) on a MyIQ thermocycler (Bio-Rad, Hercules, CA) and quantified using MyIQ software (Bio-Rad) that analyzes the $C_t$ value of real-time PCR data with the $\Delta\Delta C_t$ method for fold induction and $\Delta C_t$ method for normalized expression. *HPRT*, a housekeeping gene with constant expression, was used to normalize input cDNA.

### *In Vivo 4T1 Orthotopic Breast Cancer Model*

BALB/c mice were inoculated orthotopically in the mammary fat pad with $10^4$ 4T1 cells per mouse. Mice (18 per group) were treated daily with PBS or with PCPA [10 mg/kg, intraperitoneally (i.p.), 5 days a week] for 28 days. Primary tumor growth was monitored once a week with a caliper, and the volume was then calculated using the formula $d^2 \times D/2$, where $d$ and $D$ are the short and the long diameters, respectively. For evaluation of lung micrometastases, clonogenic assays were performed on day 28: lungs were removed from each mouse, minced, digested in 5 ml of an enzyme mix containing 1× Hank's balanced salt solution (Lonza, Basel, Switzerland), 1 mg/ml collagenase type IV (Worthington, Lakewood, NJ), and 6 U/ml elastase (Roche), and incubated for 75 minutes at 4°C on a platform rocker. After incubation, samples were filtered through and plated at different dilutions (1:2, 1:10, and 1:100) onto 10-cm tissue culture dishes in DMEM–10% FBS containing 10 μg/ml thioguanine (Sigma, Saint Louis, MO) for clonogenic growth. After 14 days of incubation at 37°C, tumor cells, which are thioguanine-resistant, formed individual colonies representing micrometastases that were fixed with methanol and stained with Giemsa (Sigma). Lung metastases were also evaluated on formalin-fixed paraffin-embedded sections stained by hematoxylin-eosin, by two operators, blindly.

### *In Vivo MDA-MB-231 Orthotopic Breast Cancer Model*

Immunodeficient NOD/SCID/IL-2Rγ$^{null}$ (NSG) mice (12 per group) were inoculated with $2.5 \times 10^6$ MDA-MB-231-GFP cells in the mammary fat pad and treated daily with vehicle (PBS) or with PCPA (10 mg/kg, i.p., 5 days a week) for 9 weeks. Growth of primary tumors was evaluated every 5 days with a caliper, and the average weight at the end of the experiments was also determined. To evaluate metastatic spread to the lungs, at the end of treatment, lungs were fixed in paraformaldehyde, embedded in paraffin, and stained with hematoxylin-eosin. Tissue slices were evaluated blindly by a pathologist and scored for metastatic infiltration (+1 = 0-15% infiltration; +2 = 15-30% infiltration; +3 = 30-60% infiltration; +4 = >60% infiltration). To evaluate lung infiltration by GFP positivity, the right superior lung lobe was dissociated by collagenase I to a single-cell suspension and analyzed by flow cytometry. Briefly, right superior lung lobe was excised and washed twice with PBS; 10 mg of lung was minced into pieces, resuspended in 1 ml of collagenase I solution [10 ml of PBS added to 20 mg of collagenase type I (Roche), 0.1 g of BSA, 10 μl of 1 M $CaCl_2$, and 10 μl of 1 M $MgCl_2$], and incubated at 37°C for 1 hour rocking. A cell strainer was used to divide dissociated cells from undigested tissue; then, cells were spun down, washed twice with PBS, and resuspended in appropriate medium for flow cytometry analyses.

### *In vivo Model of Hematogenous Metastatic Dissemination*

Five-week-old female immunocompromised mice (CB17-SCRF) were obtained from Taconic (Germantown, NY) and housed in a germ-free barrier. At 6 weeks of age, animals were anesthetized with 100 mg/kg ketamine and 20 mg/kg xylazine administered by i.p. route and successively inoculated in the left ventricle of the heart with MDA-MB-231 cells [$25 \times 10^4$ in 100 μl of serum-free DMEM/F12 (Invitrogen)]. Cell inoculation was performed using a 30-gauge needle connected to a 1-ml syringe. The delivery of the cell suspension in the systemic blood circulation was validated by the co-injection of blue fluorescent 10-μm polystyrene beads (Invitrogen, Molecular Probes). Mice were left untreated or treated with PCPA (10 mg/kg, i.p.; 24 hours before cell inoculation and at days 0, 1, and 2 post-cell injection). Organs were harvested and prepared as described below, and tissue sections were inspected blindly for single cancer cells and tumor foci. The homogeneous and numerically consistent distribution of the beads in adrenal glands and

lungs collected at necropsy and inspected by fluorescence microscopy was used as discrimination criteria for the inclusion of animals in the studies. Additional details concerning the intracardiac inoculation of cancer cells used here were previously reported [35–37]. All experiments were conducted in accordance with National Institutes of Health guidelines for the humane use of animals. All protocols were approved by the Drexel University College of Medicine Institutional Animal Care and Use Committee.

### *Tissue Processing*

Bones and soft-tissue organs were collected and fixed in 4% paraformaldehyde solution (Electron Microscopy Sciences, Hatfield, PA) for 24 hours and then transferred into fresh formaldehyde for an additional 24 hours. Soft tissues were then placed either in 30% sucrose for cryoprotection or 1% paraformaldehyde for long-term storage. Bones were decalcified in 0.5 M EDTA (Fisher Scientific, Leicestershire, United Kingdom) for 7 days followed by incubation in 30% sucrose. Tissues were maintained at 4°C for all the steps mentioned above and frozen in OCT medium (Sakura Finetek, Torrance, CA) by placement over dry ice–chilled 2-methylbutane. Serial sections of 80-μm thickness were obtained using a Microm HM550 cryostat. Femur and tibia in each knee joint were cut entirely through, resulting in approximately 32 sections per specimen available for analysis. For the analysis of lungs, three representative sections per organ were analyzed and five randomly selected microscopic fields (×10) per section were inspected for single cancer cells and tumor foci.

### *Fluorescence Microscopy and Morphometric Analysis of Metastases*

Fluorescent images of skeletal metastases were acquired using a Zeiss AX70 microscope (Carl Zeiss, Oberkochen, Germany) connected to a Nuance Multispectral Imaging System (CRI, Guelph, Ontario). Digital images were analyzed and processed with the Nuance Software (v. 2.4). Microscope and software calibration for size measurement was performed using a TS-M2 stage micrometer (Oplenic Optronics, Hangzhou, China).

### *Immunohistochemistry on Frozen Sections*

Tumor fragments were embedded in OCT compound, snap frozen, and stored at −80°C. Slides were fixed in acetone and air dried, rinsed in MeOH/3% $H_2O_2$ to block endogenous peroxidase activity, washed in PBS, and blocked in 10% fetal calf serum. Slides were covered with the primary Ab (rat anti-mouse E-cadherin; Calbiochem, San Diego, CA) for 1 hour and washed three times in PBS, followed by incubation with the secondary antibody (HRP-conjugated) and HRP-conjugated streptavidin (Sigma). Reactivity was revealed with 3,3′-diaminobenzidine. Sections were counterstained with Mayer's hematoxylin, dehydrated in graded alcohol (70%, 95%, and 100% ethanol), and mounted in BDH mounting medium (Merck Eurolabs, VWR, West Chester, PA).

### *Statistical Analysis*

Data (means ± SD, two or three experiments) were analyzed for statistical significance by unpaired, two-tailed Student's *t* test. *P* values < .05 were considered statistically significant.

## Results

### *In Vitro Effects of PCPA or Slug/LSD1 Silencing on Migration and Invasion of TNBC Cells*

In a recent study, we showed that blocking the interaction of Slug with LSD1 by treatment with PCPA inhibited the migration and invasion of tumor cell lines of different histologic and genetic backgrounds [34]. Moreover, the effects of PCPA were phenocopied by RNAi-dependent Slug or LSD1 down-regulation [34]. Since expression of Slug appears to be important for the invasive properties of breast cancer cells [25,30], we assessed the effects of PCPA or Slug/LSD1 silencing for migration, invasion, and EMT marker expression of TNBC MDA-MB-231 and BT-549 cell lines. As shown in Figure 1, *A* and *B*, wound-healing assays revealed that treatment with PCPA markedly inhibited migration of MDA-MB-231 cells; likewise, PCPA-treated MDA-MB-231 cells were less invasive than the untreated counterpart, as indicated by the marked decrease in the number of cells migrating from the upper to the lower chamber through a Matrigel layer (Figure 1*D*). Of interest, PCPA-dependent inhibition of MDA-MB-231 cell migration or invasion was not due to suppression of cell proliferation because growth rates of untreated and PCPA-treated cells are undistinguishable (Figure 1*C*). The inhibitory effects of PCPA on invasion and migration of MDA-MB-231 cells correlated with changes in the expression of epithelial and mesenchymal markers detected by real-time PCR (Figure 1*E*); expression of E-cadherin and plakoglobin that is directly repressed by Slug [15,29] was enhanced in PCPA-treated cells and similar increases were noted for occludin and desmoplakin. By contrast, expression of the mesenchymal marker N-cadherin was decreased, whereas there were no changes in the levels of vimentin. Of interest, treatment with PCPA also induced changes in the expression of other EMT regulators: expression of Twist was markedly decreased, whereas levels of Snail were increased; no significant changes in Zeb1 or Zeb2 expression were noted (Figure 2*A*). The changes in E-cadherin and N-cadherin expression in PCPA-treated MDA-MB-231 cells were confirmed by Western blot analysis (Supplementary Figure 1).

The effect of PCPA on Slug/Snail-regulated gene expression programs is thought to depend, at least in part, on its ability to disrupt the interaction between the N-terminal SNAG repressor domain of Slug/Snail and the histone demethylase LSD1 protein that is critical for Slug/Snail-dependent transcription repression [31,38]. Thus, the effects of PCPA should be phenocopied by Slug or LSD1 silencing.

To test this hypothesis, we generated Slug- or LSD1-silenced MDA-MB-231 cells and assessed their migration, invasion, and EMT marker expression profile in comparison to the scramble-transduced counterpart. Indeed, Slug or LSD1 down-regulation (Figure 3*A*) phenocopied the effects of PCPA by inhibiting migration of MDA-MB-231 cells in wound-healing assays (Figure 3, *C* and *D*) and suppressing their invasion when seeded onto Matrigel-coated Boyden chambers (Figure 3*E*). Like PCPA-treated cells, Slug- or LSD1-silenced MDA-MB-231 cells showed a significant increase in the expression of E-cadherin, occludin, and desmoplakin and a decrease in N-cadherin levels (Figure 3*F*); by contrast, expression of vimentin did not change in Slug- or LSD1-silenced cells (Figure 3*F*). Like PCPA treatment, Slug silencing led to a marked decrease in the expression of Twist and to increased Snail expression, whereas levels of Zeb1 and Zeb2 did not change (Figure 2*A*). The decrease in Twist expression may explain, at least in part, the effects of Slug silencing on migration and invasion since Twist-silenced MDA-MB-231 cells exhibited an impairment in motility (wound-healing assay) and invasion (Matrigel invasion assay) compared to the parental cell line (Supplementary Figure 2). Of interest, Slug silencing appears to be more effective than LSD1 silencing in inhibiting migration and invasion ($P = .043$) of MDA-MB-231 cells and in modulating the expression of EMT markers, especially E-cadherin (Figure 3*F*). Like

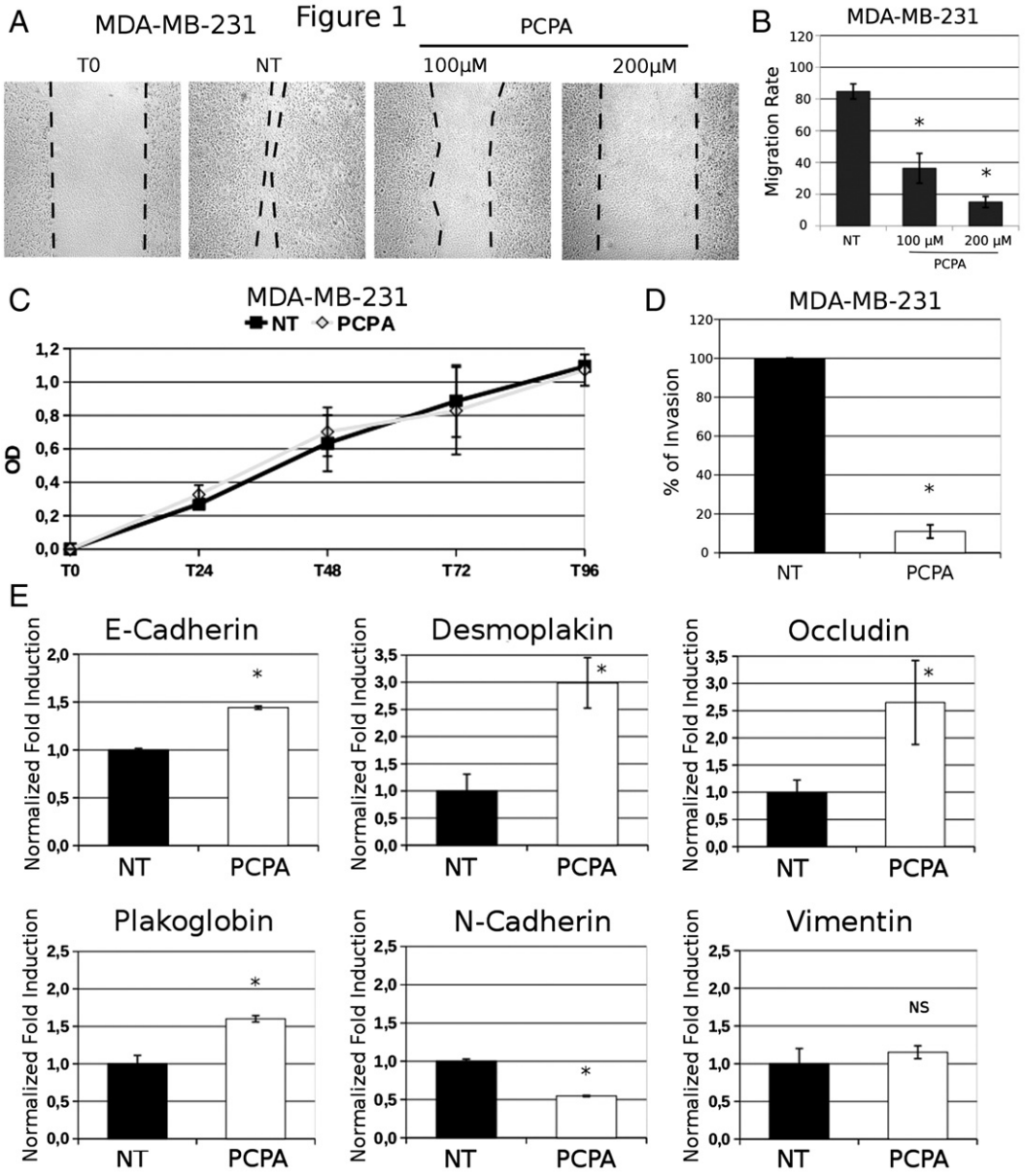


**Figure 1.** Effect of PCPA on migration, invasion, proliferation, and phenotype of TNBC MDA-MB-231 cells. Photomicrographs (A) and migration rates (B) in wound-healing assays of PCPA-treated (48 hours) MDA-MB-231 cells. (C and D) 3-(4,5-dimethylthiazol-2-yl)-2,5-diphenyltetrazolium bromide and invasion assays (expressed as percentage inhibition compared to untreated cells taken as 100) of PCPA-treated MDA-MB-231 cells. (E) Histograms of EMT marker expression (mean + SD; three independent experiments) detected by real-time qPCR in MDA-MB-231 cells treated with PCPA (12 hours). Changes in mRNA levels are all statistically significant except for vimentin.

PCPA-treated cells, proliferation of Slug- or LSD1-silenced MDA-MB-231 cells was undistinguishable from that of the scramble-transduced counterpart (Figure 3*B*).

Similar experiments were carried out using the TNBC BT-549 cell line (Supplementary Figures 3 and 4). Compared to untreated cells, PCPA-treated BT-549 cells (Supplementary Figure 3) showed a decrease in migration and invasion and modulation of EMT marker expression similar to that of PCPA-treated MDA-MB-231 cells. Likewise, Slug- or LSD1-silenced BT-549 cells also exhibited decreased invasion and migration and changes in EMT marker expression (Supplementary Figure 4) very similar to those observed in Slug- or LSD1-silenced MDA-MB-231 cells.

### *In vivo Effects of PCPA in an Orthotopic Model of Murine Metastatic Breast Cancer*

To investigate whether treatment with PCPA has anti-metastatic effects, initial experiments were carried out using an orthotopic model of mouse breast cancer 4T1 cells injected in the mammary fat pad of syngeneic mice.

First, we assessed the *in vitro* effects of PCPA on migration, invasion, and EMT marker expression of 4T1 breast cancer cells. As shown in Supplementary Figure 5, *A* to *D*, treatment with PCPA inhibited 4T1 cell migration and invasion, but the effects were less potent than in MDA-MB-231 and BT-549 cells (compare Supplementary Figure 5 with Figure 1 and Supplementary Figure 2).

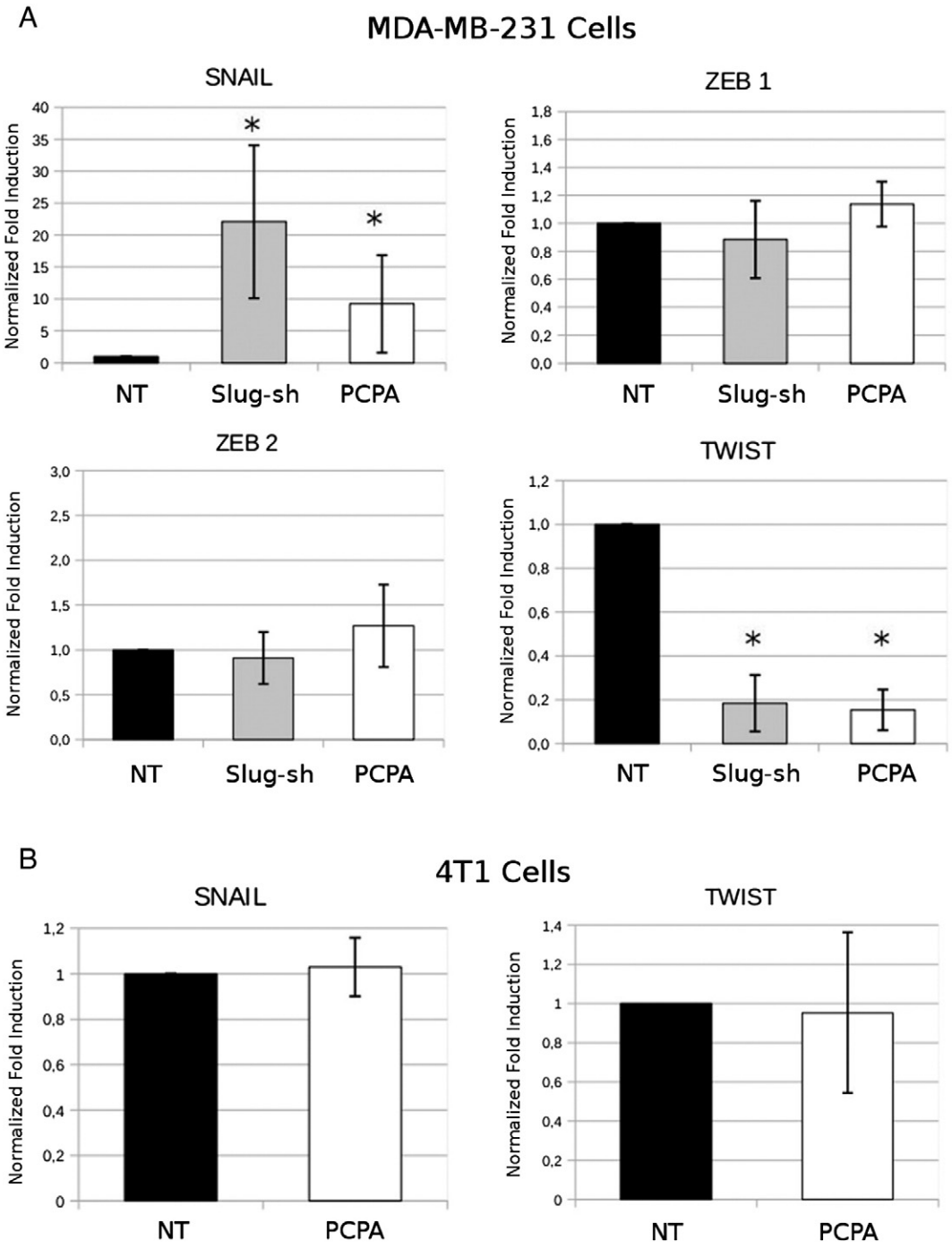


**Figure 2.** Effect of PCPA or Slug silencing on EMT-regulator expression in breast cancer lines. Histograms (mean + SD; three independent experiments) show EMT-regulator expression in PCPA-treated (24 hours) or Slug-silenced MDA-MB-231 and in PCPA-treated 4T1 cell lines detected by real-time PCR. Asterisk denotes statistically significant changes in expression compared to controls.

Likewise, treatment with PCPA induced a modest increase [detected by semiquantitative reverse transcription (RT)–PCR] in the expression of epithelial markers E-cadherin, occludin, and desmoplakin and a decrease in the levels of the mesenchymal marker vimentin (Supplementary Figure 5*E*). PCPA treatment did not induce changes in Snail or Twist mRNA levels (Figure 2*B*).

Then, BALB/c mice ($n = 36$) were injected in the mammary fat pad with 4T1 breast cancer cells ($10^4$ cells per mouse), which metastasize spontaneously to the lungs. Twenty-four hours after tumor cell injection, 18 mice were treated with PCPA (10 mg/kg per day for 28 consecutive days; i.p.) and 18 with vehicle (PBS) only; all mice were sacrificed at the end of the treatment. As shown in Figure 4, PCPA-treated mice showed a decrease in primary tumor growth statistically significant up to 21 days (Figure 4*A*) and, more importantly, a reduced number of lung metastases (Figure 4*B*) evaluated by clonogenic assays of homogenized lung tissue taken at the end of the treatment (day 28). Of interest, the diminished migratory/invasive capacity and modulation of the EMT phenotype induced by

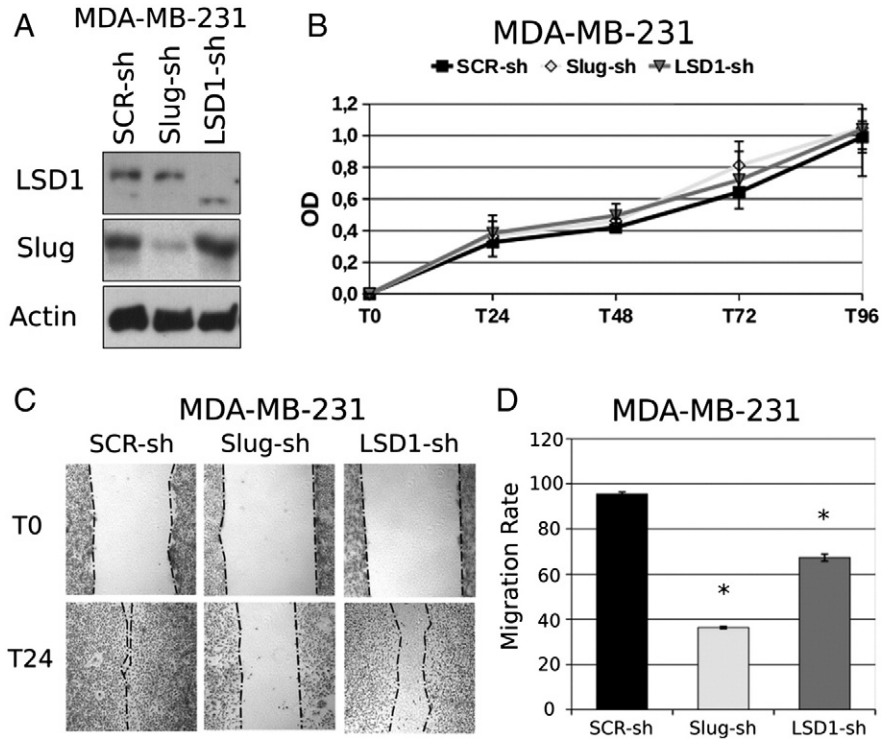


**Figure 3.** Effect of Slug or LSD1 silencing on migration, invasion, proliferation, and phenotype of TNBC MDA-MB-231 cells. (A) Western blot shows Slug or LSD1 expression in scramble or Slug/LSD1-silenced MDA-MB-231 cells. (B) 3-(4,5-dimethylthiazol-2-yl)-2,5-diphenyltetrazolium bromide assay of control or Slug/LDS1-silenced MDA-MB-231 cells. (C) Photomicrographs show wound-healing assay on Slug/LSD1-silenced MDA-MB-231 cells. (D) Histograms represent accurate measurements of migration at 0 and 48 hours of control and Slug/LSD1-silenced MDA-MB-231 cells. (E) Invasion assay: histograms show invasion (expressed as percentage inhibition compared to scramble shRNA-transduced cells taken as 100) of Slug/LSD1-silenced cells. (F) Histograms of EMT marker expression (mean + SD; three independent experiments) detected by RT-qPCR in Slug/LSD1-silenced MDA-MB-231 cells. Changes in gene expression are all statistically significant except for vimentin.

PCPA treatment *in vitro* correlated with increased E-cadherin expression in primary tumors (Figure 4, *C* and *D*). A decrease in metastases was also observed on evaluation of hematoxylin-eosin–stained lung sections from six untreated and six PCPA-treated mice (Figure 4*E*); moreover, the size of the lesions was markedly reduced in PCPA-treated mice compared to the untreated controls (Figure 4*F*).

### *In Vivo Effects of PCPA in NSG Mice Injected Orthotopically with the TNBC MDA-MB-231 Cell Line*

To assess the *in vivo* effects of PCPA in human TNBC cells, NSG mice were injected in the mammary fat pad with GFP-positive MDA-MB-231 cells and, 2 days later, treated with PCPA (10 mg/kg, i.p.; 5 days per week for 6 weeks) or with vehicle only. Tumor volume was measured every 5 days, and mice were sacrificed when tumor size of control mice was 1.8 to 2.0 $cm^3$. Then, we determined the weight of local tumors and lungs and examined the infiltration of MDA-MB-231 cells in the lungs by detection of GFP-positive cells and by morphologic examination of tissue sections. Compared to controls, treatment with PCPA induced a statistically significant decrease in tumor volume, tumor and lung weight, and lung infiltration (GFP positivity and Giemsa staining; Figure 5).

### *Effects of PCPA Treatment or Slug Silencing on Homing and Colonization of MDA-MB-231 Cells in Bone and Lungs*

These experiments were undertaken to determine whether PCPA treatment impairs the lodging of human breast cancer cells to the skeleton from the hematogenous circulation. To this end, stably fluorescent MDA-MB-231 cells were converted into CTCs by direct delivery into the left heart ventricle of immunocompromised mice. Seventy-two hours after inoculation, animals were sacrificed and evaluated for disseminated tumor cells (DTCs) in the distal femur and proximal tibia, which were inspected throughout the entire bone thickness by obtaining serial frozen sections. Compared to control animals, mice treated with PCPA (10 mg/kg, i.p.; 24 hours before cell inoculation and at days 0,1, and 2 post-cell injection) showed a dramatic decrease in the number of DTCs. Similar results were obtained by inoculating Slug-silenced MDA-MB-231 cells (Figure 6*A*). Interestingly, a reduction in DTCs was not observed on inspection of the lungs in the same animals (Figure 6*B*).

To ascertain the long-term effects of the observed DTC reduction on the growth of skeletal tumors, additional mice inoculated with MDA-MB-231 cells and treated as described above were allowed to progress for 15 days post-inoculation. When these mice were sacrificed and inspected for fluorescent tumor foci in the knee joint, control animals showed large tumors encompassing more than 80% of tibiae's and femora's tissue sections, whereas PCPA-treated mice displayed an involvement of only approximately 50%. Even more striking were the results obtained with Slug-silenced MDA-MB-231 cells; on intracardiac inoculation, these cells generated tumors involving less than 10% of bone sections (Figure 6*C*). A quantification of the overall bone involvement in each experimental group confirmed the significant reduction in skeletal tumor growth of either PCPA-treated or Slug-silenced MDA-MB-231 human breast cancer cells (Figure 6, *D* and *E*).

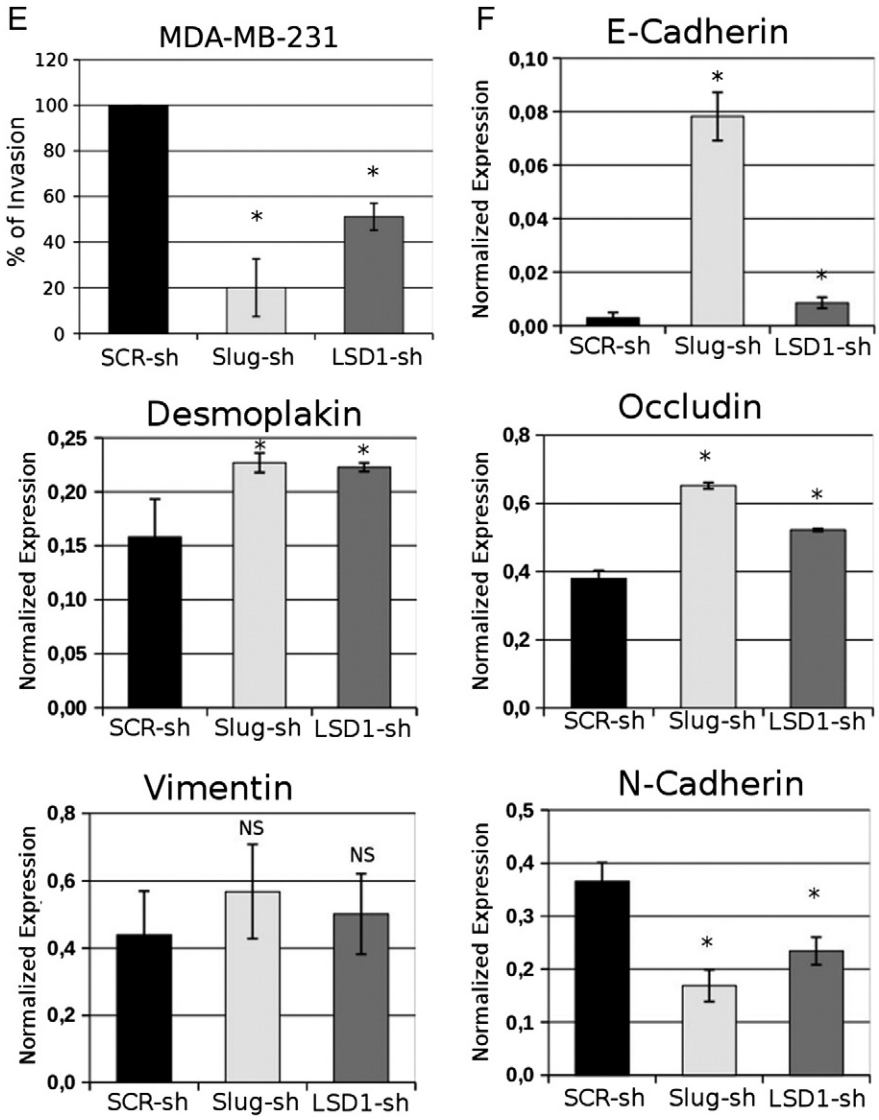


**Figure 3.** (*continued*).

## Discussion

Recent studies have shown that the transcription repression function of Snail/Slug that is essential for the EMT-promoting effects depends, in part, on the interaction of the N-terminal SNAG domain of Snail/Slug with the amine oxidase domain of the chromatin-modifying protein LSD1 [31,38]. On the basis of this finding, we showed that disrupting the interaction between Slug and LSD1 by treatment with the MAO/LSD1 inhibitor PCPA suppresses the migration and invasion of cancer cells of different origin and genetic background [34].

In this study, PCPA treatment or Slug silencing were used to investigate the requirement of Slug for the migration, invasion, and metastatic spread of TNBC cell lines. We selected this model because TNBC has a high propensity to metastasize and shows high expression of Snail and Slug, and EMT markers are readily detectable in breast cancer CTCs [5,7,8,24,25].

We show here that PCPA treatment or Slug/LSD1 silencing suppressed the migration and invasion of TNBC MDA-MB-231 and BT-549 cells without inhibiting their proliferation. Moreover, PCPA treatment or Slug/LSD1 silencing induced an increase in the levels of E-cadherin and other epithelial markers whose expression is typically downregulated during the EMT process [14]. By contrast, expression of the mesenchymal marker N-cadherin was downregulated in both TNBC cell lines, whereas levels of vimentin were only downregulated in BT-549 cells. Slug silencing appears to inhibit migration and invasion of MDA-MB-231 cells and to induce E-cadherin expression more effectively than LSD1 silencing (Figure 3); this probably reflects the ability of Slug to function, in part, through LSD1-independent transcription repressor complexes involving distinct protein domains [39]. Of interest, PCPA treatment or Slug silencing also affected the expression of the EMT regulator Twist and Snail; in particular, Twist expression was markedly decreased, whereas levels of Snail were increased (Figure 2*A*).The decreased expression of Twist appears to be biologically relevant as Twist-silenced MDA-MB-231 cells exhibit impaired motility and invasion compared to parental cells (Supplementary Figure 2).

The increase in Snail expression may depend on PCPA- or Slug silencing–induced reversal of Slug transcription repression since a functional E-box is present in the Snail promoter [40]; the decrease in the levels of Twist may be due to indirect mechanisms through inhibition of a TF positively regulating Twist expression. These results suggest that the decrease in expression/activity of Slug and

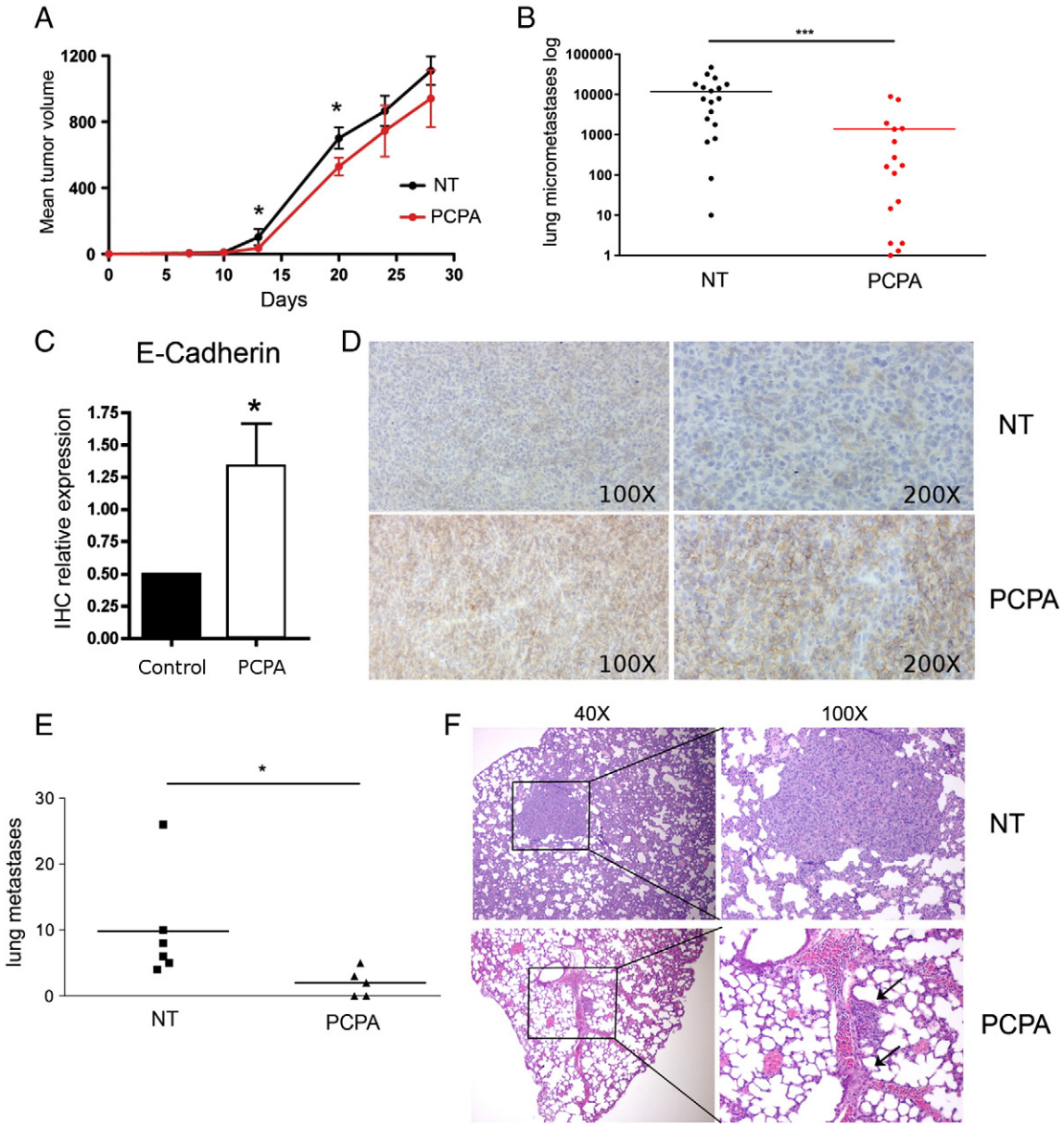


**Figure 4.** *In vivo* effects of PCPA in the 4T1 mouse breast cancer model. (A) Primary tumor volume and (B) Lung metastases (counted by clonogenic assay; see Materials and Methods section for details) in untreated or PCPA-treated BALB/c mice orthotopically injected with 4T1 breast cancer cells. Graphs show pooled data of two (A) or three (B) experiments each performed with six mice per group. (C) E-cadherin expression in primary tumor samples. Five random fields for each sample (five tumors per group) were evaluated blindly under a bright-field microscope by two operators and a score of 1 to 3 was assigned. Histogram shows mean + SD of E-cadherin expression in the control and PCPA-treated groups. (D) Representative immunihistochemistry images of E-cadherin staining. (E) Number of lung metastases detected by hematoxylin-eosin staining of formalin-fixed paraffin-embedded sections. (F) Representative images of lung sections from untreated and PCPA-treated mice bearing 4T1 tumors; ×40 and ×100 enlargements are shown. Arrows indicate two small metastases inside or in close proximity to the vessels.

Twist is not compensated by maintaining basal levels of Zeb1 and Zeb2 and even increasing Snail expression. Incidentally, the increase in expression of Snail would be less important for the effect of PCPA that functions by blocking the Snail/Slug-LSD1 interaction. In aggregate, these data strongly suggest that Slug and Twist have a predominant role among the EMT regulators in controlling the EMT process in the TNBC cell lines used here, consistent with the high expression of Slug and Twist in the highly aggressive TNBC subtypes [7,25].

Snail expression appears also to be required for *in vitro* invasion and lymph node metastasis of MDA-MB-231 cells [41]; however, the cells failed to form lung metastases and it is unknown if Twist expression was also affected by Snail silencing [41].

The *in vivo* effects of PCPA treatment were investigated in syngeneic or immunodeficient mice orthotopically injected with murine 4T1 or human MDA-MB-231 breast cancer cells, respectively, or after intracardiac injection of MDA-MB-231 cells in immunodeficient mice.

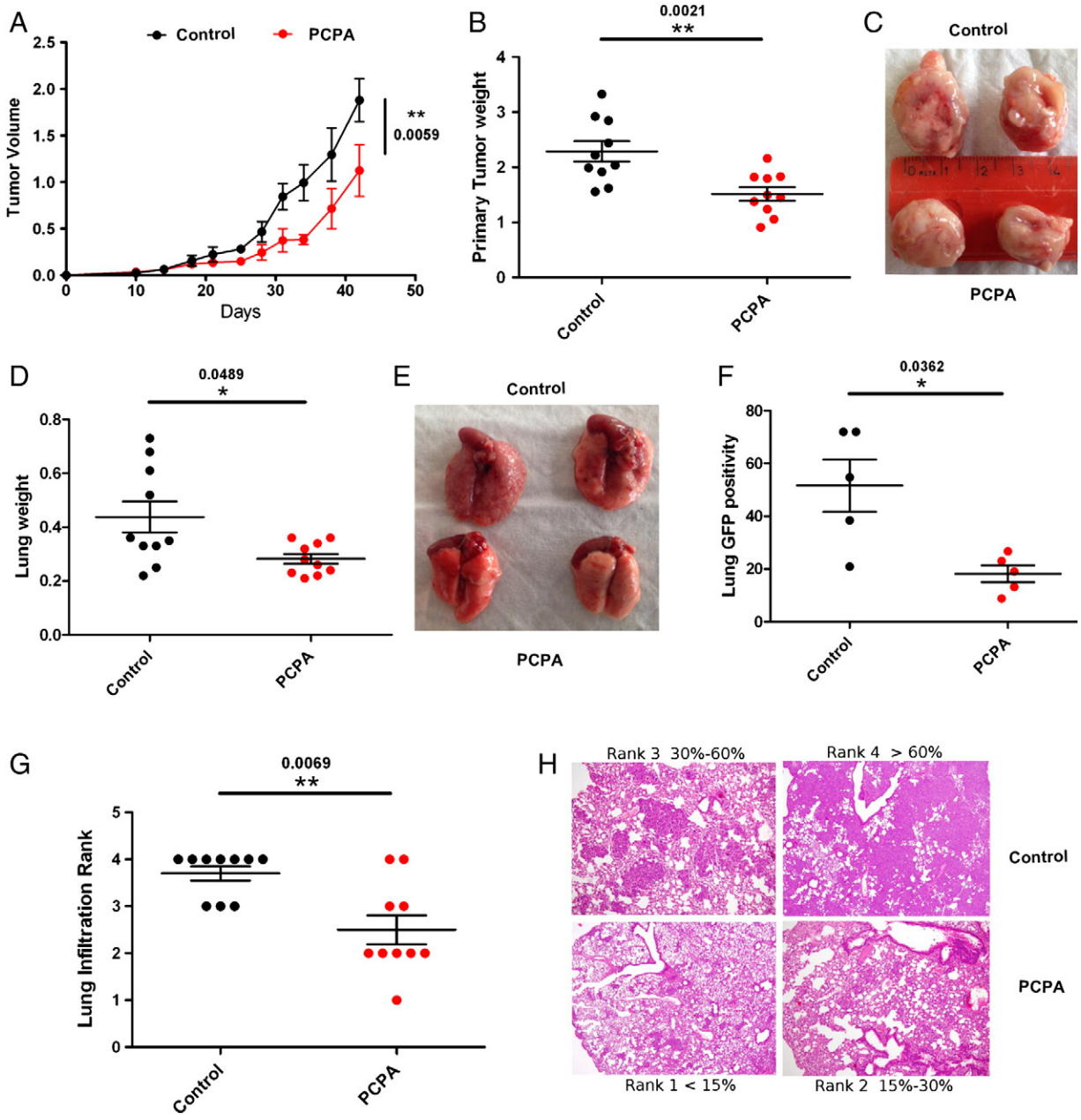


**Figure 5.** Effects of PCPA on tumor growth and lung metastases of GFP-positive MDA-MB231 cells orthotopically injected in NSG mice. (A) Tumor volume. (B and C) Tumor weight and size. (D and E) Lung weight and size. (F) Lung GFP positivity. (G and H) Lung infiltration of control or PCPA-treated samples.

In each of these models, PCPA treatment had anti-metastatic effects as indicated by decreased lung infiltration in mice orthotopically injected in the mammary fat pad and reduced bone localization in mice inoculated with MDA-MB-231 cells in the left ventricle.

In the 4T1 model, treatment with PCPA had somewhat modest effects likely because Slug plays a less important role than Twist in controlling the EMT in these cells [20,42] and Twist expression was not decreased after PCPA treatment (Figure 2*B*).

In the orthotopic model with MDA-MB-231 cells injected in immunodeficient NSG mice, treatment with PCPA markedly suppressed colonization of tumor cells to the lungs as indicated by a significant decrease in lung weight and tumor cell infiltration determined by GFP positivity and morphology (Figure 4). Of interest, local tumors of PCPA-treated mice were smaller and had a more compact and rounded appearance than those of the untreated counterpart; this may reflect constraints on local growth caused by an increase in cell adhesion and a decrease in local infiltration, although *in vivo* effects of PCPA on MDA-MB-231 cell proliferation and survival cannot be excluded. These effects are in excellent correlation with the inhibition of *in vitro* migration and invasion of MDA-MB-231 cells induced by PCPA treatment and by Slug or LSD1 silencing; moreover, they also support the concept that the metastasis-inhibitory effects of PCPA depend on disruption of the Slug/Snail-LSD1 interaction that is essential for transcription repression of E-cadherin expression [31,34,38].

In the model of intracardiac inoculation of MDA-MB-231 cells, PCPA treatment or Slug silencing markedly suppressed homing and metastasis to the bone but had no effect on homing or metastasis to the lungs. These findings are consistent with Slug/LSD1-specific effects regulating the bone-homing abilities of

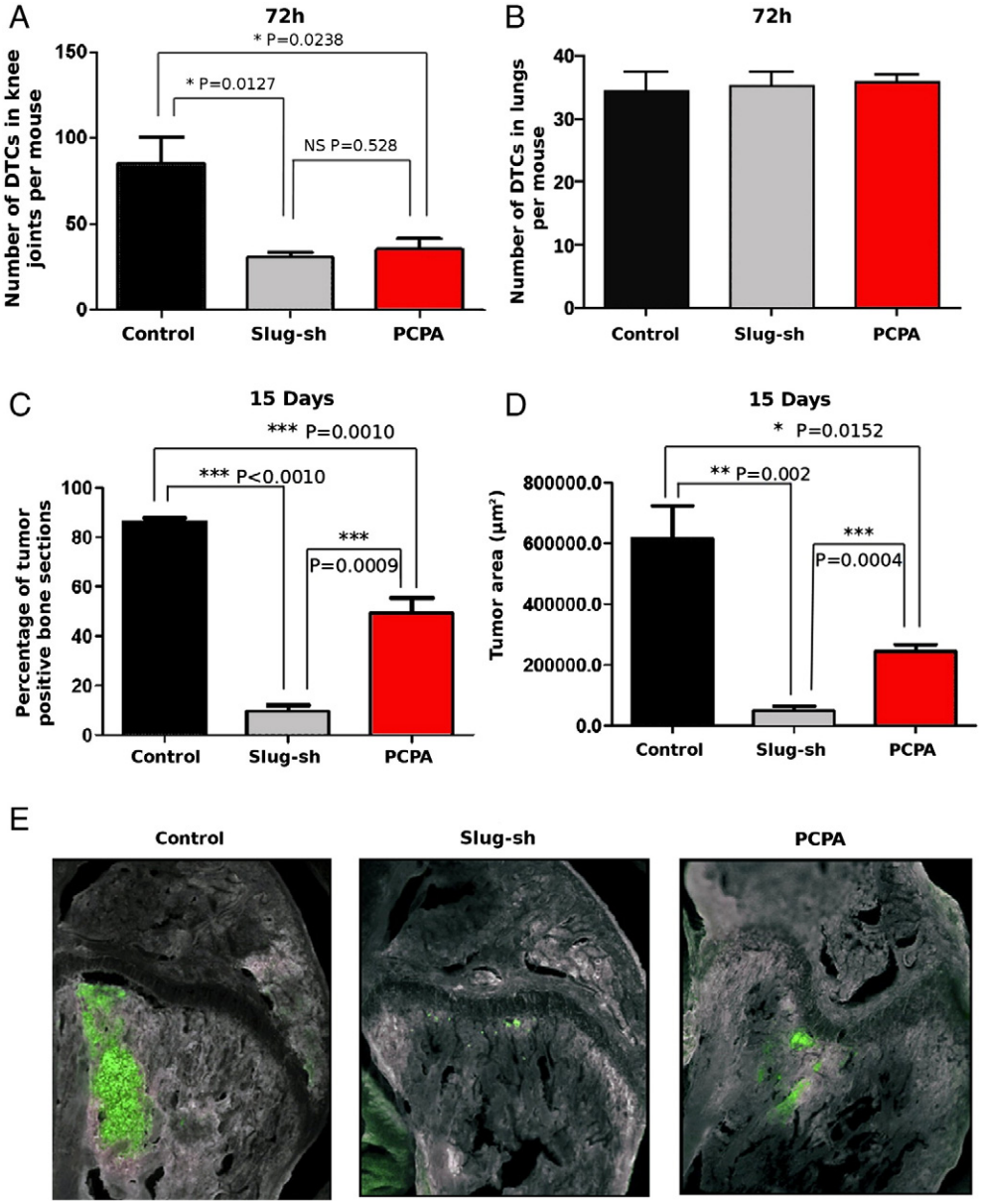


**Figure 6.** Effect of PCPA or Slug silencing on homing and colonization of MDA-MB-231 cells to the skeleton. (A and B) Number of bone (A) or lung (B) DTCs in untreated or PCPA-treated NOD/SCID mice inoculated intracardiacally with GFP-positive MDA-MB-231 cells or in mice inoculated with Slug-silenced GFP-positive MDA-MB-231 cells. (C and D) GFP-positive tissue sections (C) or tumor areas (D and E) in untreated or PCPA-treated NOD/SCID mice inoculated intracardiacally with GFP-positive MDA-MB-231 cells or in mice inoculated with Slug-silenced cells and examined 15 days post-inoculation; one-way analysis of variance test. A value of $P \leq .05$ was deemed significant.

MDA-MB-231 breast cancer cells. Furthermore, the significant reduction in the size of skeletal lesions generated by cells in which Slug expression was continuously suppressed suggests that this TF promotes tumor growth in the bone microenvironment.

However, the inhibition of MDA-MB-231 lung metastasis by PCPA treatment in the orthotopic model contrasts with a lack of effect in the intracardiac model; this suggests that inhibition of the Slug/LSD1-regulated EMT program by PCPA treatment may preferentially impair the intravasation step leading to a decrease in the number of CTCs more than affecting their extravasation as DTCs in the lung microenvironment.

In summary, this study suggests that treatment with PCPA or with other inhibitors of Slug/LSD1-regulated EMT may serve as an adjuvant therapy for patients with TNBC in whom the primary tumor has been ablated by surgery or radiation. Moreover, the finding that PCPA has tumor-inhibitory effects in the bone supports the concept that treating existing skeletal lesions with this drug may impair metastatic progression.

Supplementary data to this article can be found online at http://dx.doi.org/10.1016/j.neo.2014.10.006.

## References

[1] Peto R, Davies C, Godwin J, Gray R, Pan HC, Clarke M, Cutter D, Darby S, McGale P, and Taylor C, et al (2012). Comparisons between different polychemotherapy regimens for early breast cancer: meta-analyses of long-term outcome among 100,000 women in 123 randomized trials. *Lancet* **379**, 432–444.

[2] Davies C, Godwin J, Gray R, Clarke M, Cutter D, Darby S, McGale P, Pan HC, Taylor C, and Wang YC, et al (2011). Relevance of breast cancer hormone receptors and other factors to the efficacy of adjuvant tamoxifen: patient-level meta-analysis of randomised trials. *Lancet* **378**, 771–784.

[3] Cuzick J, Sestak I, Baum M, Buzdar A, Howell A, Dowsett M, and Forbes JF (2010). ATAC/LATTE investigators. Effect of anastrozole and tamoxifen as adjuvant treatment for early-stage breast cancer: 10-year analysis of the ATAC trial. *Lancet Oncol* **11**, 1135–1141.

[4] Gianni L, Dafni U, Gelber RD, Azambuja E, Muehlbauer S, Goldhirsch A, Untch M, Smith I, Baselga J, and Jackisch C, et al (2011). Treatment with trastuzumab for 1 year after adjuvant chemotherapy in patients with HER2-positive early breast cancer: a 4-year follow-up of a randomised controlled trial. *Lancet Oncol* **12**, 236–244.

[5] Turner NC and Reis-Filho JS (2013). Tackling the diversity of triple-negative breast cancer. *Clin Cancer Res* **19**, 6380–6388.

[6] Shah SP, Roth A, Goya R, Oloumi A, Ha G, Zhao Y, Turashvili G, Ding J, Tse K, and Haffari G, et al (2012). The clonal and mutational evolution spectrum of primary triple-negative breast cancers. *Nature* **486**, 395–399.

[7] Lehmann BD, Bauer JA, Chen X, Sanders ME, Chakravarthy AB, Shyr Y, and Pietenpol JA (2011). Identification of human triple-negative breast cancer subtypes and preclinical models for selection of targeted therapies. *J Clin Invest* **121**, 2750–2767.

[8] Yu M, Bardia A, Wittner BS, Stott SL, Smas ME, Ting DT, Isakoff SJ, Ciciliano JC, Wells MN, and Shah AM, et al (2013). Circulating breast tumor cells exhibit dynamic changes in epithelial and mesenchymal composition. *Science* **339**, 580–584.

[9] Martin-Belmonte F and Perez-Moreno M (2012). Epithelial cell polarity, stem cells and cancer. *Nat Rev Cancer* **12**, 23–38.

[10] Thiery JP, Acloque H, Huang RY, and Nieto MA (2009). EMT in development and disease. *Cell* **139**, 871–890.

[11] Prasad CP, Rath G, Mathur S, Bhatnagar D, Parshad R, and Ralthan R (2009). Expression analysis of E-cadherin, Slug and GSK3β in invasive ductal carcinoma of breast. *BMC Cancer* **9**, 2407–2419 325.

[12] Giroldi LA, Bringuier PP, de Weijert M, Jansen C, von Bohkoven A, and Schalken JA (1997). Role of E boxes in the repression of E-cadherin expression. *Biochem Biophys Res Commun* **241**, 453–458.

[13] Hennig G, Behrens J, Truss M, Frish S, Reichmann E, and Birchmeier W (1995). Progression of carcinoma cells is associated with alterations in chromatin structure and factor binding at the E-cadherin promoter in vivo. *Oncogene* **11**, 475–484.

[14] Cano A, Pérez-Moreno MA, Rodrigo I, Blanco MJ, del Barrio MG, and Portillo F (2000). The transcription factor Snail controls epithelial-mesenchymal transitions by repressing E-cadherin expression. *Nat Cell Biol* **2**, 76–83.

[15] Hajra KM, Chen DY, and Fearon ER (2002). The SLUG zinc-finger protein represses E-cadherin in breast cancer. *Cancer Res* **62**, 1613–1618.

[16] Eger A, Aigner K, Sonderegge S, Dampier B, Oehler S, Schreiber M, Berx G, Cano A, Beug H, and Foisner R (2005). DeltaEF1 is a transcriptional repressor of E-cadherin and regulates epithelial plasticity in breast cancer cells. *Oncogene* **24**, 2375–2385.

[17] Comijn J, Berx G, Vermassen P, Verscheneren K, van Grunsven L, Bruyneel E, Mareel M, Huylebroeck D, and van Roy F (2001). The two-handed E box binding zinc finger protein SIP1 downregulates E-cadherin and induces invasion. *Mol Cell* **7**, 1267–1278.

[18] Gupta PB, Kuperwasser C, Brunet JP, Ramaswamy S, Kuo WL, Gray JW, Naber SP, and Weinberg RA (2005). The melanocyte differentiation program predisposes to metastasis after neoplastic transformation. *Nat Genet* **37**, 1047–1054.

[19] Catalano A, Rodilossi S, Rippo MR, Caprari P, and Procopio A (2004). Induction of stem cell factor/c-Kit/slug signal transduction in multidrug-resistant malignant mesothelioma cells. *J Biol Chem* **279**, 46706–46714.

[20] Vitali R, Mancini C, Cesi V, Tanno B, Mancini M, Bossi G, Zhang Y, Martinez RV, Calabretta B, Dominici C, and Raschellà G (2008). Slug (SNAI2) down-regulation by RNA interference facilitates apoptosis and inhibits invasive growth in neuroblastoma preclinical models. *Clin Cancer Res* **14**, 4622–4630.

[21] Casas E, Kim J, Bendesky A, Ohno-Machado L, Wolfe CJ, and Yang J (2011). Snail2 is an essential mediator of Twist1-induced epithelial mesenchymal transition and metastasis. *Cancer Res* **71**, 245–254.

[22] Guo W, Keckesova Z, Donaher JL, Shibue T, Tischler V, Reinhardt F, Itzkovitz S, Noske A, Zürrer-Härdi U, and Belli G, et al (2012). Slug and Sox9 cooperatively determine the mammary stem cell state. *Cell* **148**, 1015–1028.

[23] Alves CC, Carneiro F, Hoefler H, and Becker KF (2009). Role of the epithelial-mesenchymal transition regulator Slug in primary human cancers. *Front Biosci (Landmark Ed)* **14**, 3035–3050.

[24] Martin TA, Goval A, Watkins G, and Jiang WG (2005). Expression of the transcription factors snail, slug, and twist and their clinical significance in human breast cancer. *Am Surg Oncol* **12**, 488–496.

[25] Storci G, Sansone P, Trere D, Tavolari S, Taffurelli M, Ceccarelli C, Guarnieri T, Paterini P, Pariali M, and Montanaro L, et al (2008). The basal-like breast carcinoma phenotype is regulated by *SLUG* gene expression. *J Pathol* **214**, 25–37.

[26] Shioiri M, Shida T, Koda K, Oda K, Seike K, Nishimura M, Takano S, and Miyazaki M (2006). Slug expression is an independent prognostic parameter for poor survival in colorectal carcinoma patients. *Br J Cancer* **94**, 1816–1822.

[27] Shih JY, Tsai MF, Chang TH, Chang YL, Yuan A, Yu CY, SB Lin, Liou GY, ML Lee, and Chen JJ, et al (2005). Transcription repressor slug promotes carcinoma invasion and predicts outcome of patients with lung adenocarcinoma. *Clin Cancer Res* **11**, 8070–8078.

[28] Olmeda D, Montes A, Moreno-Bueno G, Flores JM, Portillo F, and Cano A (2008). Snai1 and Snai2 collaborate on tumor growth and metastasis properties of mouse skin carcinoma cell lines. *Oncogene* **27**, 4690–4701.

[29] Bailey CK, Mittal MK, Misra S, and Chaudhuri G (2012). High motility of triple-negative breast cancer cells is due to repression of plakoglobin gene by metastasis modulator protein SLUG. *J Biol Chem* **287**, 19472–19486.

[30] Xue J, Lin X, Chiu WT, Chen YH, Yu G, Liu M, Feng XH, Sawaya R, Medema RH, Hung MC, and Huang S (2014). Sustained activation of SMAD3/SMAD4 by FOXM1 promotes TGF-β–dependent cancer metastasis. *J Clin Invest* **124**, 564–579.

[31] Lin Y, Wu Y, Li J, Dong C, Ye X, Chi YI, Evers BM, and Zhou BP (2010). The SNAG domain of Snail1 functions as a molecular hook for recruiting lysine-specific demethylase 1. *EMBO J* **29**, 1803–1816.

[32] Baron R, Binda C, Tortorici M, McCammon JA, and Mattevi A (2011). Molecular mimicry and ligand recognition in binding and catalysis by the histone demethylase LSD1-CoREST complex. *Structure* **19**, 212–220.

[33] Lee MG, Wynder C, Schmidt DM, McCafferty DG, and Shiekhattar R (2006). Histone H3 lysine 4 demethylation is a target of nonselective antidepressive medications. *Chem Biol* **13**, 563–567.

[34] Ferrari-Amorotti G, Fragliasso V, Esteki R, Prudente Z, Soliera AR, Cattelani S, Manzotti G, Grisendi G, Dominici M, and Pieraccioli M, et al (2013). Inhibiting interactions of lysine demethylase LSD1 with Snail/Slug blocks cancer cell invasion. *Cancer Res* **73**, 235–245.

[35] Russell MR, Liu Q, and Fatatis A (2010). Targeting the α receptor for Platelet-Derived Growth Factor as a primary or combination therapy in a preclinical model of prostate cancer skeletal metastasis. *Clin Cancer Res* **16**, 5002–5010.

[36] Jamieson-Gladney WL, Zhang Y, Fong AM, Meucci O, and Fatatis A (2011). The chemokine receptor $CX_3CR1$ is directly involved in the arrest of breast cancer cells to the skeleton. *Breast Cancer Res* **13**, R91.

[37] Liu Q, Russell MR, Shahriari K, Jernigan DL, Lioni MI, Garcia FU, and Fatatis A (2013). Interleukin-1β promotes skeletal colonization and progression of metastatic prostate cancer cells with neuroendocrine features. *Cancer Res* **73**, 3297–3305.

[38] Lin T, Ponn A, Hu X, Law BK, and Lu J (2010). Requirement of the histone demethylase LSD1 in Snai1-mediated transcriptional repression during epithelial-mesenchymal transition. *Oncogene* **29**, 4896–4904.

[39] Molina-Ortiz P, Villarejo A, MacPherson M, Santos V, Montes A, Soucheinytskyi S, Portillo F, and Cano A (2012). Characterization of the SNAG and SLUG domains of Snail2 in the repression of E-cadherin and EMT induction: modulation by serine 4 phosphorylation. *PLoS One* **7**, e36132.

[40] Peiró S, Escrivà M, Puig I, Barberà MJ, Dave N, Herranz N, Larriba MJ, Takkunen M, Francí C, and Muñoz A, et al (2006). Snail1 transcriptional repressor binds to its own promoter and controls its expression. *Nucleic Acids Res* **34**, 2077–2084.

[41] Olmeda D, Moreno-Bueno G, Flores JM, Fabra A, Portillo F, and Cano A (2007). SNAI1 is required for tumor growth and lymph node metastasis of human breast carcinoma MDA-MB-231 cells. *Cancer Res* **67**, 11721–11731.

[42] Yang J, Mani SA, Donaher JL, Ramaswamy S, Itzykson RA, Come C, Savagner P, Gitelman I, Richardson A, and Weinberg RA (2004). Twist, a master regulator of morphogenesis, plays an essential role in tumor metastasis. *Cell* **117**, 927–939.